Effect of the Shear and Volume Fraction on the Aggregation and Breakup of Particles

Teresa Serra and Xavier Casamitjana
Dept. of Environmental Sciences, University of Girona, 17071 Girona, Catalonia, Spain

The aggregation and breakup of particles in a Couette flow system were studied for different values of the shear rate (G) and the volume fraction of particles ϕ_o. After a certain time, an initial distribution of 2- μm-dia. latex particles achieves the steady state, reflecting the balance between coagulation and fragmentation forces. Higher G values shift the steady state to smaller aggregate sizes. For a fixed value of G, when ϕ_o increases, the steady-state size increases if the flow is laminar and decreases if the flow is turbulent. The population balance model proposed describes simultaneous coagulation and fragmentation during shear flocculation. A power dependence between the breakage rate coefficient and the shear rate was found. The model is adjusted by using two parameters: the probability of success for collisions α and the effective breakup coefficient for shear fragmentation B'_{eff} depends on both G and ϕ_o, while α is nearly constant.

Introduction

It is well known that, as a result of collisions, particles form aggregates that have higher effective sizes than primary particles. This increase in size is found to be especially relevant in lakes or in the sea, where aggregates, as pointed out by Casamitjana and Schladow (1993), can account for the removal of particles in the epilimnion. Particles in lakes are in a continuous process of aggregation and breakup until eventually the steady-state size is reached. The final size of the aggregates seems to depend on the shear rate and the volume fraction (Serra et al., 1997). Aggregates play an important role in volcanic eruptions, where aggregate formation, initiated in the atmosphere, induces a premature fallout of fine-grained ash. As a result, when the aggregates are absorbed by the ocean, the settling velocity is higher than would be expected for dispersed ash particles (Weisner et al., 1995). At the same time, aggregation introduces modifications in the effective surfaces of the particles (Krishnappan et al., unpublished), which can be important carriers of pollutants that adhere to them. As the surface area of the aggregates increases, more pollutants can be absorbed.

Different experiments carried out with sediment particles (Lick and Lick, 1988; Tsai et al., 1987) and with latex particles (Oles, 1992; Pandya and Spielman, 1983) show that the aggregation of particles is a dynamic process. The particle size distribution at any particular time is determined by the rates at which individual particles aggregate and disaggregate. The rates of the aggregation and disaggregation processes are different and the average size of the distribution increases or decreases according to whether the aggregation mechanism is higher or lower than the disaggregation mechanism. The steady state is reached when the disaggregation process balances the aggregation process.

The physical processes that control particle aggregation have been well known since the pioneering work of Smoluchowski (1917). However, the disaggregation processes are not so well understood. The aggregation rate depends on the rate at which collisions occur and on the probability of cohesion of particles after collision. The disaggregation rate depends on the shear rate and the probability of disaggregation after collision. Burban et al. (1989) proposed a model to explain the aggregation of sediments that takes into account the effect of the shear, but not the breakup. Based on the experiments of Oles (1992), Spicer and Pratsinis (1996) proposed a model for the breakup process; however, as Oles used a fixed value for ϕ_o, the effect of ϕ_o in the breakup process was not predictable. Covering a wide spectrum in the laminar and turbulent flows. Serra et al. (1997) showed that both G and ϕ_o are important in the breakup of the aggregates.

In the present study, primary particles with a diameter of 2 μm are introduced in a Couette shear flow. As no differ-

Correspondence concerning this article should be addressed to T. Serra.

ences exist between particle and fluid densities, the only relevant mechanism in the collision frequency is the shear rate G. A physical model is used in order to understand the effect of G and ϕ_o in the aggregation and breakup process. The model is adjusted by using two different parameters: the probability of success for collisions α, and the effective breakup coefficient for shear fragmentation, B'_{eff}. The values obtained for these two parameters are discussed and compared with values found by Spicer and Pratsinis (1996).

Experimental Results

Aggregation and disaggregation was performed in a Couette flow system (Figure 1) with the inner cylinder rotating at a constant speed and the outer cylinder at rest. The inner cylinder, with a diameter of 163 mm, was made of stainless steel to avoid corrosion. The outer cylinder, with a diameter of 193 mm, was made of Plexiglas so the fluid would be visible. The height of the cylinder was 360 mm. Suspensions of latex particles were prepared in 1.29 M NaCl solution in ultrapure water at different volume fractions (ϕ_o) ranging from 2.5×10^{-5} to 10.0×10^{-5}. The diameter of the latex particles was $d_o = 2.00 \pm 0.06$ μm. To avoid sedimentation effects, the density of the solution was set at the same value as that of the latex particles, $\rho_p = 1.055$ g/cm^3. Therefore, differential settling will be negligible in the process of aggregation. In addition, as a result of this salt dilution, the electric double layer was highly reduced to an approximate value of the Debye-Hückel length of 10^{-8} m. Samples were taken from the Couette flow system and analyzed by a laser particle size analyzer that scanned the sample. A more complete description of the whole system can be found in Serra et al. (1997).

The angular velocity at which transition to turbulence takes place can be estimated from van Duuren's equation (van Duuren, 1968), and was found to be approximately 98 rpm (Serra et al., 1997). The angular velocities used in this study ranged from 40 rpm to 211 rpm, therefore covering the transition from laminar to turbulent flow. The value of the shear rate G was estimated to range from $G = 25$ s^{-1} to 195 s^{-1} and was determined depending on whether the flow was laminar to turbulent, as was explained by Serra el al. (1997). Transition from laminar to turbulent flow was estimated to occur at $G = 58$ s^{-1}.

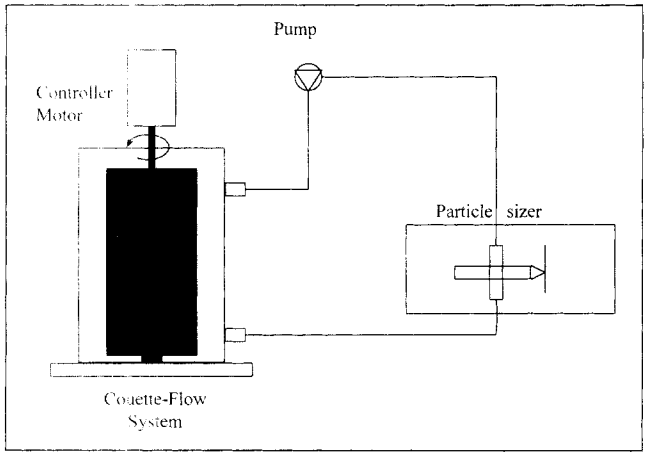

Figure 1. Experimental setup.

The relationship between viscous forces and thermal forces is given by the Peclet number,

$$Pe = \frac{3\pi\mu G d_o^3}{4k_B T} \tag{1}$$

where μ is the fluid viscosity, d_o is the diameter of the primary particles, k_B is the Boltzmann constant, and T is the temperature. In all the cases studied, the Peclet number was found to be higher than 120. This ensures that aggregation due to Brownian movement can be neglected compared with the shear-induced aggregation (Oles, 1992).

Evolution of the dimensionless diameter d/d_o with the dimensionless time t^* for different G, when the initial volume fraction is $\phi_o = 2.5 \times 10^{-5}$, is plotted in Figure 2. As the characteristic diameter, d, we use the median of the size distribution with respect to the aggregate volume. t^* depends on G, and ϕ_o, as $t^* = tG\phi_o$. This dimensionless time represents a normalized number of collisions taking place in the system (Oles, 1992). At the beginning of the experiments shown in Figure 2, at small t^*, d/d_o scaled well with t^*. At larger t^*, breakup is more pronounced until it balances the aggregation process, and the steady state is then reached. For all the cases studied in Figure 2, the steady-state size is reached for $t^* \cong 7$. But taking into account that t^* depends on the product Gt, this means that the steady state size is reached sooner when G increases (Serra et al., 1997). In addition, it is found that, the larger G is, the faster the aggregation occurs. As a result, the system reaches the steady state more rapidly and the final size of the dimensionless diameter of the aggregates is smaller. This behavior is supported by other authors such as Oles (who worked with latex particles),

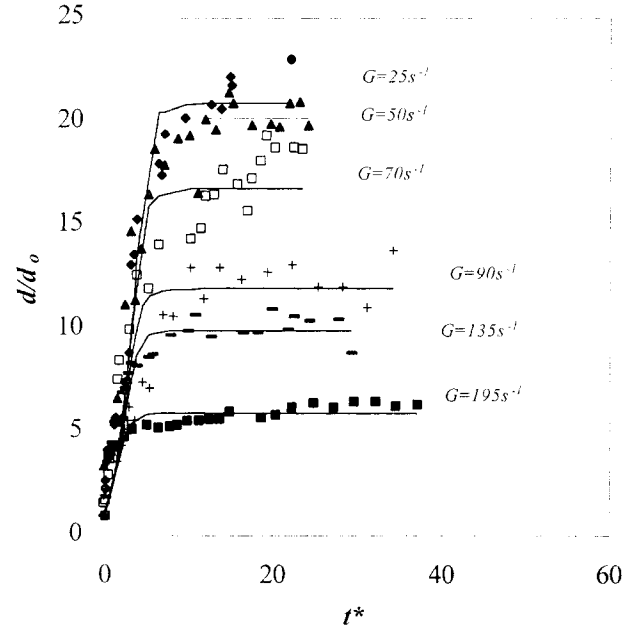

Figure 2. Evolution of d/d_o versus the dimensionless time t^* at different shear rate values and at $\phi_o = 2.5 \times 10^{-5}$.

Points correspond to the experimental data and lines correspond to the model predictions.

Lick and Lick (1988), Burban et al. (1989), and Tsai et al. (1987), who worked with sediment particles.

Figure 3 depicts the relationship between the normalized diameter at the steady state, $(d/d_o)_{est}$, and ϕ_o at different G values. Three regimes or zones can be differentiated. The first one corresponds to value of $\phi_o < 6 \times 10^{-5}$, approximately (regime A). Here, the value of $(d/d_o)_{est}$ depends on G, but not on ϕ_o. This regime was also found by Oles (1992). When $\phi_o > 6 \times 10^{-5}$, two new regimes can be identified depending on the value of G. When G is less than 50 s^{-1}, if ϕ_o increases, the aggregation is enhanced and the final diameter of the aggregates increases (regime B in Figure 3). However, when $G > 50$ s^{-1}, if ϕ_o increases $(d/d_o)_{est}$ decreases (regime C in Figure 3). Higher values of ϕ_o give more collisions between the particles in the suspension. For higher values of G, collisions between aggregates will have enough energy to cause breakup. For lower values of G, collisions between the particles will not have enough energy to break them. This is in accordance with the work of Tsai et al. (1987) and Lick and Lick (1988), using sediment particles; however, these authors did not study the aggregation/breakup process at the range of low shear rate values, as was done in our case. It is important to point out that the transition from regime B to regime C coincides with the transition from laminar flow to turbulent flow.

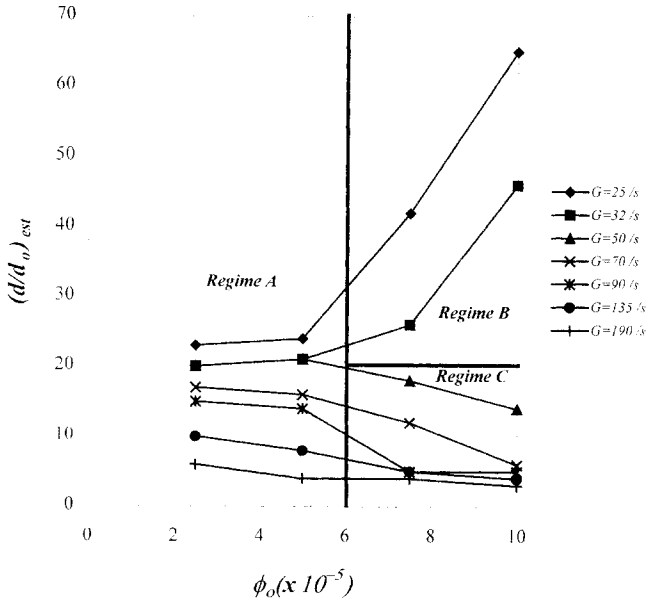

Figure 3. Final diameter of the aggregate.

Normalized to the diameter of the primary particles, $(d/d_o)_{est}$, for different volume fractions, ϕ_o, at different values of the shear rate, G.

Description of the Model

To model the rate of change of particles of a given size due to the process of aggregation and breakup, Lick and Lick (1988) proposed the following expression:

$$\frac{dn_k}{dt} = \frac{1}{2}\sum_{i+j=k}\alpha\beta_{ij}n_i n_j - n_k\sum_{i=1}^{\infty}\alpha\beta_{ik}n_i - B_k n_k + \sum_{j=k+1}^{\infty}\gamma_{jk}B_j n_j - n_k\sum_{i=1}^{\infty}\alpha'\beta_{ik}n_i + \sum_{j=k+1}^{\infty}\gamma_{jk}n_j\sum_{i=1}^{\infty}\alpha'\beta_{ij}n_i \qquad (2)$$

where n_k is the number of particles per unit volume corresponding to size class k, characterized by the diameter d_k. The first two terms on the righthand side of the equation are used to model the aggregation processes, while the others are used for the disaggregation processes.

The first term on the righthand side represents the rate at which particles of size class k are formed from collisions between particles of size classes i and j. The second term on the righthand side represents the loss of particles of size class k due to collisions with the rest of particles. α is the probability of success for a collision between two particles. β_{ij} is the collision frequency function for particles of size classes i and j and depends on the physical mechanism of the interparticle contacts. The third term on the righthand side of Eq. 2 represents the loss of size class k particles, giving particles with lower diameters. This disaggregation is due to the effect of the shear rate on the particles. The fourth term on the righthand side of Eq. 2 represents the rate of increase of size class k due to the disaggregation of bigger particles caused by the shear rate. The quantity γ_{jk} is the breakage distribution function defining the volume fraction of the fragments of size class k coming from the disaggregation of a particle of size class j. The fifth term on the righthand side represents the loss of particles of size class k due to unsuccessful collisions with all the other particles. The last term on the righthand side represents the rate of increase of particles of size class k after unsuccessful collisions between particles of size classes i and j, where j is greater than k. Finally, α' represents the probability of disaggregation after collisions.

Contact between particles in water can occur by three different processes: Brownian motion, fluid shear, and differential settling. The collision frequency function for the Brownian motion is

$$\beta_{ij} = \frac{2}{3}\frac{k_B T}{\mu}\frac{(d_i + d_j)^2}{d_i d_j} \qquad (3)$$

The collision frequency function for the fluid shear is

$$\beta_{ij} = \frac{G}{6}(d_i + d_j)^3 \qquad (4)$$

The collision frequency function for the differential settling is

$$\beta_{ij} = \frac{\pi g}{72\mu}(d_i + d_j)^2|\Delta\rho d_i^2 - \Delta\rho_j d_j^2| \qquad (5)$$

where g is the acceleration due to gravity and $\Delta\rho = \rho_l - \rho$ is the difference in the effective density of the particle of size class i and the density of the water.

Volume conservation has been assumed in the model. That means that, when a particle of size class i aggregates with a

particle of size class j, a particle of size class k is given whose volume is

$$V_k = V_i + V_j \tag{6}$$

The main difficulty in using Eq. 2 for modeling the aggregation and breakup processes is that even approximate values of α' are unknown at the present time. However, if an effective rate of breakage is defined as,

$$B_{k,\text{eff}} = B_k + \sum_{i=1}^{\infty} \alpha' \beta_{ik} n_i \tag{7}$$

Eq. 2 can be written in the form,

$$\frac{dn_k}{dt} = \frac{1}{2} \sum_{j+i=k} \alpha \beta_{ij} n_i n_j - n_k \sum_{i=1}^{\infty} \alpha \beta_{ik} n_i - B_{k,\text{eff}} n_k + \sum_{j=k+1}^{\infty} \gamma_{kj} B_{j,\text{eff}} n_j \tag{8}$$

In Eq. 7 $B_{k,\text{eff}}$ accounts for linear breakup and the breakup resulting from collisions between two clusters or nonlinear breakup. Obviously, $B_{k,\text{eff}}$ should increase with ϕ_o as the number of collisions and the rate of nonlinear breakup increase with ϕ_o. Also, the rate of linear breakup B_k is expected to increase when G increases and therefore $B_{k,\text{eff}}$ will increase too. This will be later confirmed by the experimental results. Spicer and Pratsinis (1996) used an equation similar to Eq. 8 but they did not take into account the effect of the nonlinear breakup. In Eq. 8, the value of β was calculated from Eq. 4 because the shear is the only mechanism that induces collisions between particles, as was discussed in the experimental section.

The effective breakage rate due to the effect of G, $B_{k,\text{eff}}$, has been assumed to depend on the volume as,

$$B_{k,\text{eff}} = B'_{\text{eff}} V_k^{(1/3)} \tag{9}$$

where V_k is the volume of the particle of the size class k and B'_{eff} is the effective breakage coefficient for shear fragmentation and volume fraction fragmentation. Other authors have made similar assumptions (Spicer and Pratsinis, 1996; Kapur, 1972; Boadway, 1978; Williams, 1990) and expressed the fact that particles with a high volume are more easily broken up in a sheared flow.

The aggregation and disaggregation process occurs over a wide size range. In order to represent the whole population of particles, the size domain has been divided into 23 classes or sections that give the same number of the equations. The smallest size is the size of the primary particles, characterized by a diameter d_o and a volume V_o. The volume of the higher size class has been taken 2^{22} times V_o in order to account for the biggest aggregates formed. Also, in order to model the breakage processes it has been assumed that when a particle of size class j disaggregates due to the effect of shear rate, it will split in a well-shaped distribution of particles covering the range from size class l, corresponding to the primary particles, to j, thus causing a normal distribution in the continuous space. Therefore γ_{jk} has been calculated from,

$$\gamma_{jk} = \frac{V_j}{V_k} \frac{\binom{j}{k}}{\sum_{k=0}^{j} \binom{j}{k}} \tag{10}$$

A similar assumption has also been used by Spicer and Pratsinis (1996).

Model Results

Given an initial distribution of particles, Eqs. 7 and 8 have been solved using a finite difference scheme for each one of the 23 size classes until the steady-state size was reached. Simulations were done for different values of ϕ_o, and G, in order to cover all the cases with available experimental data. In order to test the model a special routine that calculates the total mass of the system, and verifies conservation of the mass, was coupled to it. In order to test the model we have added a routine to the model that computes the value $\sum_k dV_k/dt$. In each run this value was estimated to be less than 10^{-11}, ensuring the volume conservation and, given that ρ_p was constant, mass conservation as well.

Table 1 summarizes the model results. The two first columns give the values of ϕ_o and G, while the rest of the columns give the output values of the model, namely, the adjusting parameters B'_{eff} and α, and the fitting error calcu-

Table 1. Shear Rate Values, G, Collision Efficiency, α, Effective Breakage Rate Coefficient, B'_{eff} ($\times 10^{-2}$), and Fitting Errors at Different ϕ_o

$\phi_o(10^{-5})$	G	$B'_{\text{eff}}(\times 10^{-2})$	α	Fitting Error (%)
		$\phi_o(10^{-5}) = 2.5$		
	25	6.0	1	17
	32	9.5	1	14
	50	14.8	1	10
2.5	70	30.6	1	12
	90	39.8	1	18
	135	103.0	1	16
	195	323.0	1	14
		$\phi_o(10^{-5}) = 5.0$		
	25	13.2	1	16
	32	15.6	1	10
	50	27.8	1	12
5.0	70	50.9	1	13
	90	106.0	1	16
	135	207.0	1	14
	195	645.4	1	15
		$\phi_o(10^{-5}) = 7.5$		
	25	5.5	1	18
	32	32.1	1	16
	50	51.0	1	14
7.5	70	74.0	1	14
	90	525.0	1	10
	135	803.0	1	11
	195	2,803.1	1	15
		$\phi_o(10^{-5}) = 10.0$		
	25	1.0	0.4	20
	32	2.8	0.4	14
	50	139.0	1	9
10.0	70	582.0	1	14
	90	718.0	1	17
	135	19,994.4	1	14
	195	152,060.4	1	11

lated by matching the theoretical and experimental data obtained. This error varies from 10% to 20%, approximately. Also, in Figure 2 the results predicted by the model for a volume fraction $\phi_o = 2.5 \times 10^{-5}$ are compared to the experimental data obtained as described in the last paragraph.

It is instructive to represent the variations of the effective breakup coefficient for shear fragmentation B'_{eff} with G. In Figure 4a these variations are represented for the volume fractions $\phi_o = 2.5 \times 10^{-5}$ and 5.0×10^{-5}, in Figure 4b for $\phi_o = 7.5 \times 10^{-5}$, and in Figure 4c for $\phi_o = 10.0 \times 10^{-5}$. In all the cases a power relationship,

$$B'_{\text{eff}} = kG^b \tag{11}$$

as suggested by Spicer and Pratsinis (1996), fits well with experimental data. These authors suggested that b depends on the inverse of the floc strength, while k is constant.

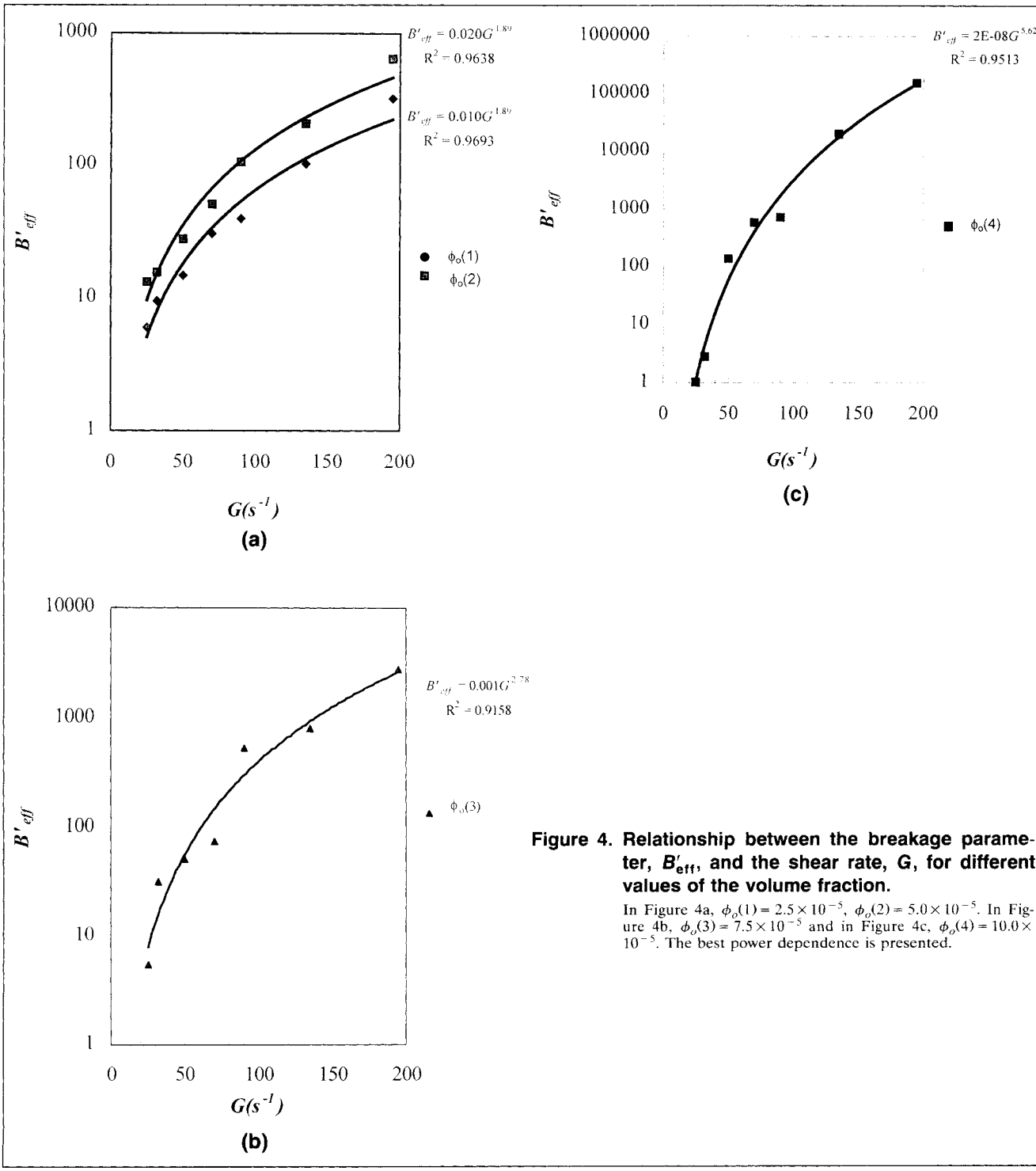

Figure 4. Relationship between the breakage parameter, B'_{eff}, and the shear rate, G, for different values of the volume fraction.

In Figure 4a, $\phi_o(1) = 2.5 \times 10^{-5}$, $\phi_o(2) = 5.0 \times 10^{-5}$. In Figure 4b, $\phi_o(3) = 7.5 \times 10^{-5}$ and in Figure 4c, $\phi_o(4) = 10.0 \times 10^{-5}$. The best power dependence is presented.

It is important to point out that the cases represented in Figure 4a correspond to the regime A (Figure 3). Here the exponent b was found to be 1.89 and seems to be independent of ϕ_o, at least for the available data. This is in accordance with the experimental observations that in this regime the value of the volume fraction does not affect the behavior of the system. For the volume fractions of 2.5×10^{-5} and 5.0×10^{-5} the obtained values of k were 0.010 and 0.020, respectively. Also, the value $b = 1.89$ agrees with the results found by Spicer and Pratsinis (1996) who modeled the experimental data of Oles (1992) corresponding to the case $\phi_o = 5.0 \times 10^{-5}$. However, as we have extended the model to cover regimes B and C (Figure 3) we will show that the values of b and k are no longer the same values found in regime A.

For the case represented in Figure 4b ($\phi_o = 7.5 \times 10^{-5}$), $b = 2.78$ and $k = 0.001$ and for the case represented in Figure 4c ($\phi_o = 10.0 \times 10^{-5}$), $b = 5.62$ and $k = 2.0 \times 10^{-8}$. These results seem to suggest that if ϕ_o is higher than 6×10^{-5} approximately (regimes B and C), the value of b increases with ϕ_o, indicating that the power dependence between B'_{eff} and G is stronger when ϕ_o increases, that is, the solution is more concentrated. Figure 5 shows the relationship between b and ϕ_o. The increase in b with ϕ_o can be explained when it is taken into account that the number of collisions increases with ϕ_o. Collisions at low G do not have enough energy to cause breakup and result in aggregation. Collisions at high G have more energy and result in breakup, in accordance with the experimental results (Figure 3), whereas the same change in the value of G causes a more pronounced change in $(d/d_o)_{\text{est}}$ at high values of ϕ_o (as 10.0×10^{-5}) than at low values of ϕ_o (as 5.0×10^{-5}).

In Table 1 it can be seen that $\alpha = 1$ for most of the simulated cases and is smaller only in some cases corresponding to regime B (Figure 3). A constant value for α with the shear rate (Table 1) is reasonable because α depends on the chemical interactions between the particles and their physical properties but not on the flow characteristics. $\alpha = 1$ indicates that the suspension was completely destabilized and that all of the collisions were successful. The complete success of all collisions is unlikely, because that would mean that collisions are unimportant in the disaggregation process, even with higher shear rate values. This behavior ($\alpha = 1$) is also found by Spicer and Pratsinis (1996), and can be attributed to the fact that colloidal aggregates have fractal structures (Lin et al., 1989; Li and Logan, 1997), which are not taken into account in the model. As was pointed out before by Jiang and Logan (1991), a higher coagulation frequency exists due to the fractal structure of the actual flocs at $\alpha = 1$. A higher value of the collision frequency might compensate for the reduction of collision efficiency. However, it is important to point out that α is a complex function of the stability of the suspension, the surface chemistry of the particles, and the structure of the aggregates or the diameter of the aggregates, as has been proposed by other authors (Burban et al., 1989). Further work should incorporate all of these contributions to the α value.

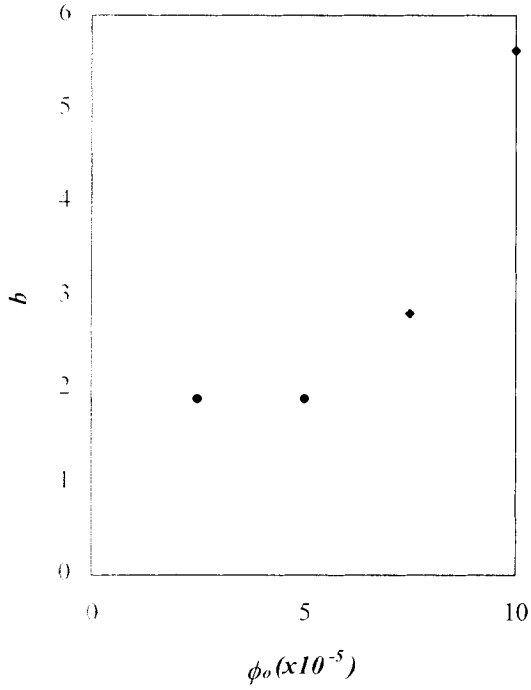

Figure 5. Relationship between b and ϕ_o.

Conclusions

An experimental study was carried out to investigate aggregation and breakup of particles in a Couette flow system with the inner cylinder rotating at a constant speed. Experiments have been conducted with suspensions of latex particles with an initial diameter of 2 μm at different values of ϕ_o. Depending on both G and ϕ_o, three different regimes were found. In the first regime, when ϕ_o is less than 6×10^{-5}, approximately (regime A in Figure 3), $(d/d_o)_{\text{est}}$ is independent of ϕ_o and depends only on G. When ϕ_o is higher, two new regimes are identified, with the final diameter of the aggregate depending on both G and ϕ_o. When G is less than 50 s^{-1}, if ϕ_o increases, the aggregation is enhanced and the final diameter of the aggregates increases (regime B in Figure 3). However, when $G > 50$ s^{-1}, if ϕ_o increases $(d/d_o)_{\text{est}}$ decreases (regime C in Figure 3). Also, the transition between these two regimes corresponds to the transition from laminar to turbulent flow.

A population balance model is used in order to understand the dynamics of the aggregation and breakup process. The model uses 2 independent parameters: the probability of success for collisions α, and the effective breakup coefficient for shear fragmentation, B'_{eff}. The parameter α depends on the chemical interactions between the particles and their physical properties but not on the flow characteristics. For this reason, α has been found to be nearly constant. The parameter B'_{eff} accounts for linear breakup and the breakup resulting from collisions between two clusters, which is nonlinear. This parameter was found to depend on both G and ϕ_o. The relationship $B'_{\text{eff}} = kG^b$ fits well with the experimental data. Different values of k and b were found for the different regimes. The value of b was found independent of ϕ_o in regime A, while it was found to be dependent on ϕ_o in regimes B and C. The value of k was found to be dependent on ϕ_o in all of the regimes.

Literature Cited

Boadway, J. D., "Dynamics of Growth and Breakage of Alum Floc in Presence of Fluid Shear," *J. Env. Eng. Div. Proc. ASCE*, **104**, 901 (1978).

Burban, P. Y., W. Lick, and J. Lick, "The Flocculation of Fine-Grained Sediments in Estuarine Waters," *J. Geophys. Res.*, **94**, 8323 (1989).

Casamitjana, X., and G. Schladow, "Vertical Distribution of Particles in Stratified Lake," *J. Environ. Eng.*, **119**, 443 (1993).

Jiang, Q., and B. E. Logan, "Fractal Dimensions of Aggregates Determined from Steady-State Size Distributions," *Environ. Sci. Technol.*, **25**, 2031 (1991).

Kapur, P. C., "Self-Preserving Size Spectra of Comminuted Particles," *Chem. Eng. Sci.*, **27**, 425 (1972).

Krishnappan, B. G., N. Madsen, R. Stephens, and E. D. Ongley, "A Field Instrument for Size Distribution of Flocculated Sediment," in press (1998).

Li, X., and B. E. Logan, "Collision Frequencies between Fractal Aggregates and Small Particles in a Turbulently Sheared Fluid," *Environ. Sci. Tech.*, **32**, 1237 (1997).

Lick, W., and J. Lick, "Aggregation and Disaggregation of Fine-Grained Lake Sediments," *J. Great. Lakes Res.*, **14**, 514 (1988).

Lin, M. Y., H. M. Lindsay, D. A. Weitz, R. C. Ball, R. Klein, and P. Meakin, "University in Colloid Aggregation," *Nature*, **339**, 360 (1989).

Oles, V., "Shear-Induced Aggregation and Breakup of Polystyrene Latex Particles," *J. Colliod Interf. Sci.*, **154**, 351 (1992).

Pandya, J. D., and L. A. Spielman, "Floc Breakage in Agitated Suspensions: Effect of Agitation Rate," *Chem. Eng. Sci.*, **38**, 1893 (1983).

Serra, T., J. Colomer, and X. Casamitjana, "Aggregation and Breakup of Particles in a Shear Flow," *J. Colloid Interf. Sci.*, **187**, 466 (1997).

Smoluchowski, M., "Versuch either Mathematischen Theorie der Koagulations Kinetis Kolloider Lösunger," *Z. Physik. Chem.*, **92**, 129 (1917).

Spicer, P. T., and S. T. Pratsinis, "Coagulation and Fragmentation: Universal Steady-State Particle-Size Distribution," *AIChE J.*, **42**, 1612 (1996).

Tsai, C. H., S. Iacobellis, and W. Lick, "Flocculation of Fine-Grained Lake Sediments due to a Uniform Shear Stress," *J. Great Lakes Res.*, **13**, 135 (1987).

van Duuren, F. A., "Defined Velocity Gradient Model Flocculator," *J. Sanitary Eng. Div.*, **4**, 6076 (1968).

Weisner, M. G. m., Y. Wang, and L. Zheng, "Fallout of Volcanic Ash to the Deep South China Sea Induced by the 1991 Eruption of Mount Pinatubo (Philippines)," *Geology*, **23**, 885 (1995).

Williams, M. M. R., "An Exact Solution of the Fragmentation Equation," *Aerosol Sci. Technol.*, **12**, 538 (1990).

Manuscript received May 28, 1997, and revision received May 26, 1998